Vibrational Energy Dynamics of Normal and Deuterated Liquid Benzene

Nak-Hyun Seong, Ying Fang, and Dana D. Dlott*

School of Chemical Sciences, University of Illinois at Urbana−Champaign, Urbana, Illinois 61801

Received: November 2, 2008; Revised Manuscript Received: December 12, 2008

Ultrafast Raman spectroscopy with infrared (IR) excitation is used to study vibrational energy dynamics of ambient temperature liquids benzene and benzene-d_6. After IR pumping of a CH-stretch or CD-stretch parent excitation, the redistribution of vibrational energy is probed with anti-Stokes Raman. Ten benzene or 12 benzene-d_6 vibrations out of 30 total have large enough cross sections to be observed. The pathways, quantum yields, and lifetimes for energy transfer among these vibrations are quantified. Using a CCl_4 molecular thermometer, we demonstrate an ultrafast Raman calorimetry method which allows measurement of the rate that benzene vibrational energy is dissipated into the bath. On the basis of energy conservation, we then determine the time-dependent dissipation of aggregate vibrational energy from the unobserved, "invisible" vibrations. During the ∼1 ps IR excitation process, vibrational energy is coherently redistributed to several vibrational modes ("coherently" means the rate is faster than $(T_2)^{-1}$ of the pumped transition). This energy is then further redistributed in an incoherent intramolecular vibrational relaxation process with a 6 ps T_1 time constant. The subsequent dynamics involve energy transfer processes accompanied by vibrational energy dissipation to the bath. This vibrational cooling process has a half-life of 30 ps in benzene and 20 ps in benzene-d_6, and thermalization is complete in ∼100 ps. The observed strongly Raman-active vibrations have about the same amount of energy per mode as the invisible vibrations. The invisible vibrational energy in benzene decays somewhat faster than the observed energy. These two decay rates are about the same in benzene-d_6.

1. Introduction

In this study, we reexamine the vibrational energy dynamics of liquid benzene using ultrafast Raman spectroscopy. We employ the same methods to study benzene-d_6 for the first time. A CH- or CD-stretch fundamental is pumped with a 1 ps duration infrared (IR) pulse. This parent excitation undergoes a fast intramolecular vibrational redistribution (IVR) process that results in energy loss with vibrational relaxation (VR) lifetime T_1. Parent VR occurs by exciting lower-energy daughter vibrations, which themselves relax until a thermalized state is achieved with a small temperature jump ΔT. Incoherent anti-Stokes Raman probing[1] is used, which quantitatively determines the instantaneous occupation number of all Raman-active vibrations simultaneously.[2,3] To infer the behavior of benzene vibrations that are not Raman-active, we simultaneously probe the vibrational cooling (VC) process by spiking the benzene with a CCl_4 molecular thermometer.[2−5] This thermometer provides a readout with high time resolution of the total quantity of dissipated energy.

Other liquids that have been studied by the IR−Raman method include H_2O,[6−13] CH_2Cl_2,[14] $CHCl_3$,[15,16] CH_3-CN,[17,18] CH_3-NO_2 and CD_3-NO_2,[5,19] pyrrole,[20,21] and CH_3-OH.[22,23] We have recently developed a substantially improved IR−Raman apparatus[5,24] that features greatly improved signal acquisition capabilities and a micro sample-handling system to study liquids such as benzene-d_6, which previously were needed in prohibitively expensive quantities.

The VC process in polyatomic liquids has traditionally been viewed as a vibrational cascade, a multistep descent down a vibrational ladder.[25] Vibrational cascade is a good description for high-lying vibrational states of diatomic molecules in condensed phases, in which a molecule such as XeF in solid Ar might be prepared in $v = 20$ and then cascade down the ladder of lower v states until cooled.[26] But with larger polyatomic molecules, IR−Raman and hot fluorescence measurements did not observe this type of successive-stepladder descent.[25] Energy from the parent excitation tended to randomize rather than descend a ladder. Recently, our group has introduced a three-stage model[5,24,27] for VC of condensed-phase molecules that is used to describe situations in which the initial excitation has enough energy for the primary decay to occur via IVR.[5,24] This model was discussed extensively in two recent publications from our group.[5,27] As depicted in Figure 1, we divide the molecular vibrational excitations into three tiers: the parent, P; the midrange levels, M; and the lower energy levels, L, along with a bath consisting of a continuum of lower-energy collective excitations. This division is based on the 1979 paper by Nitzan and Jortner.[28] The three stages are (1) The laser-excited parent vibration undergoes IVR, resulting in the excitation of many if not all lower-energy daughter vibrations. (2) The resulting M and L daughters decay. The M daughters decay by exciting L daughters with the excess energy dissipated into the bath. The L daughters decay entirely into bath excitations. (3) The second generation of L daughters that were created from M vibrations then decay into the bath. This three-stage model thus differs from a vibrational cascade in that the state created after the parent decays populates most or all of the rungs of the vibrational ladder, and there is only a single (M to L) step down the ladder.

Benzene has a high molecular symmetry, D_{6h}, and a skeletal framework more rigid than the molecules mentioned above. Raman intensity is concentrated in a rather small number (6−7) of transitions. Unlike the studies on $CHCl_3$[16] or CH_3NO_2,[5] in

* Author to whom correspondence should be addressed. E-mail: dlott@illinois.edu.

10.1021/jp809679y CCC: $40.75
Published on Web 02/02/2009

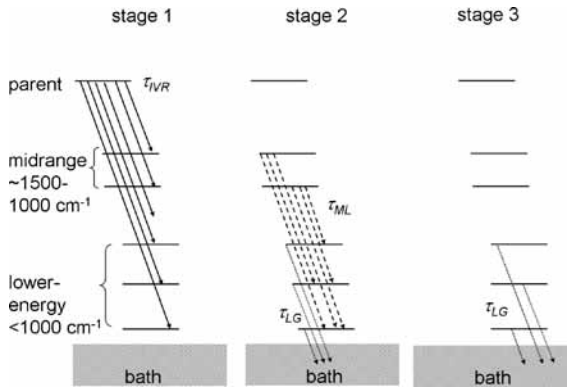

Figure 1. Schematic of the three-stage model for vibrational cooling. Stage 1: A parent vibration, P, such as a CH-stretch is excited. P undergoes a fast intramolecular redistribution consisting of a coherent transfer part on the time scale of T_2 and an incoherent IVR with lifetime τ_{IVR}. These processes populate most or all lower-energy vibrations. Stage 2: The midrange tier M undergoes vibrational relaxation (VR) with lifetime τ_{ML} by exciting lower-energy vibrations, L, plus the bath, while L undergoes VR with time constant τ_{LG} (G denotes ground vibrational state) by exciting only bath excitations. Stage 3: Second-generation lower-energy vibrations L created in stage 2 undergo relaxation with time constant τ_{LG}.

which most or even all vibrations could be probed, in benzene, much of the vibrational energy will be in Raman-inactive modes we cannot observe. One of the fundamental issues addressed in this study is, to what extent can we infer the behavior of the unseen or "invisible" vibrational energy solely from the observed transitions? To do this, we have developed an "ultrafast Raman calorimetry" method. We have a known energy input from the laser pulse, and we can total up all the observed vibrational energy and bath energy from anti-Stokes measurements of benzene and the CCl_4 molecular thermometer. On the basis of energy conservation, what remains represents the time-dependent aggregate invisible vibrational energy.

Another way of investigating the invisible vibrational energy is to closely examine the rising edges of the anti-Stokes transients. When energy is transferred from a higher- to a lower-energy vibration, there will be a component in the rising edge of the lower vibration transient that matches a component in the decay of the higher vibration. If we can identify time constants in the rising edges that do not have decay counterparts in other transients, we can infer the existence of an invisible vibration with that lifetime and might even be able to assign the vibration.

A second fundamental issue we address is whether the three-stage model is a good description of benzene VC, or does the high-symmetry rigid framework choke off some VR pathways, resulting in VC that proceeds along more specific channels than the efficient randomization that has been observed in more flexible molecules such as nitromethane,[5] methanol,[23] or glycine.[24,27]

A third fundamental issue we address is the nature of the parent state created by ultrashort IR excitation. The parent state is a "bright" state, an admixture of anharmonically coupled normal modes with energies near 3050 cm^{-1} that combine to create a strong transition dipole moment. The bright state may, in addition to CH-stretch character, have skeletal deformation and CH-bend character. In such a case, if the parent were pumped and probed with femtosecond time resolution using ultrashort IR pulses or femtosecond stimulated Raman, damped quantum beats (which are well-known in both vibronic spectroscopy,[29] and ultrafast IR spectroscopy[30]) would be observed, which would reveal the strong coupling among the states comprising the bright state. As discussed previously,[23] in our anti-Stokes experiments, IR excitation is semi-impulsive. The pulse duration (1 ps) is long compared to a vibrational period (10 fs), comparable to T_2 ($\sim$1 ps) and shorter than T_1 (6 ps), where T_2 was estimated on the basis of the 10 cm^{-1} line width of benzene, ν_1,[31] using $\Delta\nu = (\pi c T_2)^{-1}$. Thus, we probe vibrational populations in the parent and coupled states averaged over a time period, $\sim T_2$, and do not resolve quantum beats. In this case, the nature of the bright state can be investigated by looking for states other than the pumped CH-stretch that evidence an instantaneous rise ("instantaneous" means the rise is indistinguishable from the laser instrument response function). Vibrations that evidence such an instantaneous rise are said to be "coherently coupled" to the pumped CH-stretch excitation, in the sense that the redistribution occurs on timescales comparable to or faster than T_2.

Benzene vibrational energy has previously been studied in isolated molecules, liquids, and low-temperature crystals. In isolated molecules, the CH-stretch fundamentals near 3050 cm^{-1} have VR that is so slow that the states decay by IR emission.[32] The VR of several of the CH-stretch overtones[33−37] has been studied in detail. Prior studies of low-temperature crystals[34,38,39] involved indirect methods that probed the IR or Raman line widths in the frequency or time domains. Vibrational line widths in ambient liquids are ordinarily dominated by pure dephasing processes[31,40] and sometimes inhomogeneous broadening,[25] so T_1 cannot be confirmed from line width measurements. However in low-temperature isotopically pure crystals,[41] T_1 processes are believed to be dominant[42] so that T_1 can be determined from the Raman line width. In the liquid state, Fendt and co-workers[43] studied benzene with time-resolved anti-Stokes Raman; however, those studies probed only the parent relaxation process, and in fact, the parent CH-stretch lifetime was incorrectly determined, because the signals detected appear to have originated from a coherence artifact due to nonlinear light scattering.[44] Iwaki and co-workers[44] measured $T_1 = 8$ ps for the parent CH-stretch and also observed signals originating from daughter excitations at 1584, 991, and 606 cm^{-1}. CCl_4 molecular thermometer data were noisy but suggested an overall time constant for VC of $\sim$80 ps.

2. Experimental

Spectroscopic-grade benzene and perdeuterobenzene (99.9% D) were purchased from Sigma-Aldrich and used without additional purification. Raman spectra were obtained using picosecond 532 nm pulses with a bandwidth of $\sim$25 cm^{-1}, whereas the IR spectra were obtained using an FTIR spectrograph with 2 cm^{-1} resolution. The IR−Raman measurement technique has been described previously.[5] Briefly, a tunable mid-IR pulse of $\sim$1.0 ps duration, 40 cm^{-1} bandwidth, 200 μm diameter, 25 μJ (benzene), or 15 μJ (deuterobenzene) energy pumped a recirculating liquid jet 65 μm thick. The liquid samples flowed from a microjet at ambient temperature. The IR pulses were tuned to either a CH-stretch absorption near 3050 cm^{-1} or a CD-stretch absorption near 2280 cm^{-1}. A time-delayed 532 nm probe pulse of $\sim$1.0 ps duration, 25 cm^{-1} bandwidth, 80 μm diameter, and 20 μJ energy generated Raman scattering. Raman signals were detected over the −3800 to +3800 cm^{-1} range with a multichannel spectrograph and CCD detector. At each delay time, a 1 min integration was performed. The laser apparatus response measured using nonlinear light scattering in water[7,8] was a good fit to a Gaussian with 1.4 ps fwhm.

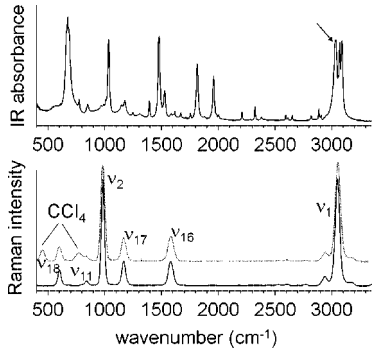

Figure 2. IR and Raman spectra of benzene and Raman spectrum of benzene with 17% CCl_4. The arrow indicates the wavenumber of the pump pulse. The Raman spectra are artificially broadened due to the 25 cm^{-1} bandwidth of the 532 nm laser pulses. Mode assignments are summarized in Table 1.

Raman spectra were obtained in pairs, a signal at the indicated positive time delay and a background obtained at negative time delay (probe precedes IR pump). The Stokes spectrum was monitored to verify that the sample did not degrade during data acquisition. Stokes and anti-Stokes signals were combined to determine quantitative occupation numbers as follows. When the occupation number of a vibration of frequency ω is n_ω and the laser frequency is ω_L, the Stokes intensity is

$$I_{ST} \propto \omega_L(\omega_L-\omega)^3[n_\omega + 1]\sigma_R \quad (1)$$

and the anti-Stokes intensity is

$$I_{AS} \propto \omega_L(\omega_L + \omega)^3 n_\omega \sigma_R \quad (2)$$

where intensity is taken to mean the integrated area of the transition. For doubly degenerate modes, eqs 1 and 2 give the total occupation number of both modes. The proportionality constant is a function of the detection system, which is the same for both Stokes and anti-Stokes measurements, and σ_R is the Raman cross section at ω_L. When $n_\omega \ll 1$, the fraction of molecules in the excited state is given by the fraction I_{AS}/I_{ST}. The detection system was corrected for its wavelength-dependent response using a calibrated blackbody source (Ocean Optics, Dunedin, FL). Each vibrational transition was fit to a Voigt line shape function using Microcal Origin software (OriginLab Corp., Northampton, MA) to determine the integrated area. The Voigt function was used because it provided an excellent fit to all the transitions and is not intended to convey specific information about vibrational dephasing.[5]

3. Results

A. Benzene. Figure 2 shows IR and Raman spectra of benzene and the Raman spectrum of benzene spiked with 17% (v/v) CCl_4. The arrow in the IR spectrum indicates the frequency of the IR pump pulses. The most intense transition near the pump pulse has been assigned to ν_{12}. In the Raman spectrum, six transitions dominate: ν_1, ν_2, ν_{11}, ν_{16}, ν_{17}, and ν_{18}. ν_1 and ν_2 are singly degenerate, and the other four are doubly degenerate, so a total of 10 modes are observed. The vibrational wavenumbers and assignments are given in Table 1. Figure 3 shows a time series of anti-Stokes spectra following IR pumping at 3063 cm^{-1}, and Figure 4 shows the time-dependence of the vibrational populations (occupation numbers) of the six observed transitions extracted from the data in Figure 3. For doubly degenerate states, the occupation number is the aggregate population. All the vibrations except ν_{11} and ν_{17} evidence an instantaneous component on the rising edge. This instantaneous component indicates that the parent "bright" state, which is excited by tuning the IR pulse into ν_{12}, consists of an admixture of ν_{12} with ν_1, ν_2, ν_{16}, ν_{18}, and possibly other states we could not observe.

Figure 5 shows a time series of anti-Stokes spectra for benzene with 17% CCl_4, and Figure 6 shows the time-dependent vibrational populations. Figure 7 compares the benzene vibrational population transients with (circles) and without (squares) CCl_4. The shorter-time vibrational populations with and without CCl_4, are similar because the sample is optically thick at the pump frequency and optically thin at the probe frequency.[2] In this limit, the number of excitations generated by the pump pulses is determined by the number of IR photons rather than the sample absorption coefficient. The benzene vibrational dynamics appear not to be noticeably affected by the presence of CCl_4 at this concentration, in agreement with previous work.[44] The smooth curves in Figure 7 are the fits to the neat benzene data using the three-stage model, as discussed below.

After the VC process is complete, the sample comes to equilibrium at a final temperature, T_f, (T_f represents an average over a spatially inhomogeneous region of the liquid pumped by the IR pulses[5]). Figure 8 shows benzene + CCl_4 anti-Stokes spectra obtained at negative delay (probe precedes pump) where the sample is at ambient temperature, and a spectrum obtained at a longer delay time after the parent excitation has thermalized. The accuracy of determining T_f for an anti-Stokes transition is greatest for higher frequency transitions with larger Raman cross sections.[45,46] We were able to determine T_f for ν_{18}, ν_2, and ν_{17} with an estimated error of 2−4 K, as shown in Figure 8, and when the results for each vibration were averaged, our determination gave $\Delta T = 40$ K. The value of ΔT would be expected to be ~15% greater in neat benzene due to the greater IR absorption coefficient at the pump wavenumber.

B. Benzene-d_6. Figure 9 shows the IR and Raman spectra of benzene-d_6 and the Raman spectrum of benzene-d_6 with 17% CCl_4. We observe the same transitions (ν_1, ν_2, ν_{11}, ν_{16}, ν_{17}, ν_{18}) as in benzene, and we see an additional CD-stretch transition, ν_{15}. Since five of these seven modes are doubly degenerate, we observe a total of 12 vibrations. The frequencies and assignments of the benzene-d_6 vibrations are given in Table 1. In benzene-d_6, an instantaneous component in the rising edge is observed in ν_1, ν_2, and ν_{15} only. The benzene-d_6 population transients with and without CCl_4 are compared in Figure 10, where the smooth curves were obtained by fitting the neat benzene-d_6 data to the three-stage model. Unlike benzene, in which CCl_4 spiking seemingly has no effect on the vibrational transients, in benzene-d_6, CCl_4 has a small effect on the ν_1 decay and a more significant effect on ν_{17}, possibly due to the near coincidence with the CCl_4 ν_3 vibration. Figure 11 is an analysis of the temperature jump ΔT for benzene-d_6 with CCl_4. This $\Delta T = 10$ K is much smaller than with benzene because both the CD-stretch absorption coefficient and the IR laser energy were smaller.

4. Discussion

A. Anti-Stokes Transients and the Three-Stage Model. An anti-Stokes Raman transient consists of three parts: a rising edge, a decay, and a longer-time plateau. The rising edge shows how the vibrational excitation became excited and is, thus, the key to understanding vibrational energy flow. The decay is determined by the vibrational lifetime, T_1, which results from fluctuating forces acting on the excitation from the surroundings,[47] consisting of other vibrations and the bath.[28] The plateau results from the bulk temperature jump, ΔT. In our analysis, we pay the greatest amount of attention to the rising edges, seeking to resolve the time constants on the rising edge and

TABLE 1

Benzene					
			source of excitation		
wavenumber (cm^{-1})	assignment	lifetime T_1 (ps)	IR pump pulse[a]	parent	M to L
3063	ν_1: ν_s (CH)	6.2	17%		
1589	ν_{16}: ν (CC)/(992 + 606)	20	28%		
1176	ν_{17}: δ_{ip} (CH)	146	0	42%	8%
992	ν_2: ring breathing	55	34%	39%	0
850	ν_{11}: δ_{oop} (CH)	125	0	0	44%
606	ν_{18}: δ_{ip} (CCC)	300	21%	19%	48%
Benzene-d_6					
			source of excitation		
wavenumber (cm^{-1})	assignment	lifetime T_1 (ps)	IR pump pulse[b]	parent	X-state[c]
2282	ν_1: ν_s (CD)	6.4	27%		
2254	ν_{15}: ν_{as} (CD)	4.5	24%		
1551	ν_{16}: ν (CC)	25	0	22%	0
937	ν_2: ring breathing	26	48%	0	0
868	ν_{17}: δ_{ip} (CD)	53	0	13%	19%
653	ν_{11}: δ_{oop} (CD)	137	0	36%	26%
578	ν_{18}: δ_{ip} (CCC)	91	0	29%	55%

[a] The absolute fraction of CH-stretch excitations generated by the IR pump pulse is 1.3% in benzene. [b] The absolute fraction of CD-stretch excitations generated by the IR pump pulse is 0.5% in benzene-d_6. [c] The lifetime of state X is 80 ps.

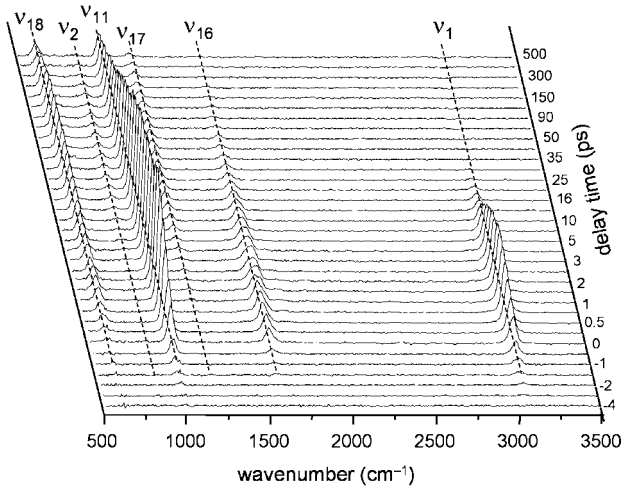

Figure 3. Time-series of benzene anti-Stokes spectra after IR pumping at 3053 cm^{-1}. Note the delay time axis is not a linear scale.

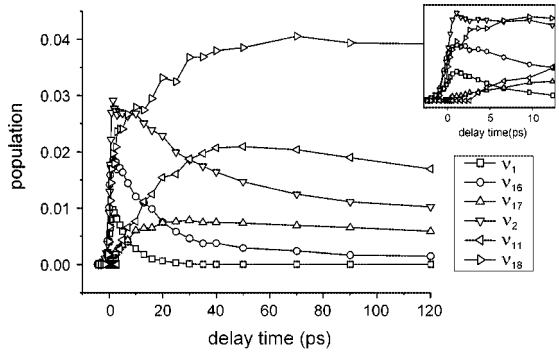

Figure 4. Population transients for benzene determined using time-dependent Stokes and anti-Stokes spectra.

identifying the process associated with a particular time constant.[27] The fastest processes are complete within 1 ps and are associated with the laser pulse duration. Any transition evidencing such a fast rising edge is taken to be part of the coherent admixture that defines the parent bright state.[2,17]

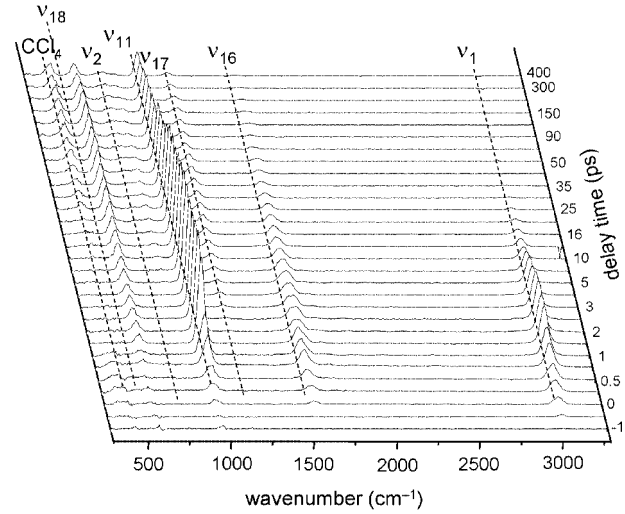

Figure 5. Time-series of anti-Stokes spectra after IR pumping at 3053 cm^{-1} from a mixture of benzene + 17% CCl_4 (v/v). Note the delay time axis is not a linear scale.

The three-stage model is depicted schematically in Figure 1. In the first stage of the VC process, the parent, P, relaxes with time constant $\tau_{IVR} = (k_{IVR})^{-1}$, so seeing this time constant on the rising edge of a midrange, M, or lower-energy, L, vibration indicates that vibration becomes excited as a result of parent IVR. During parent IVR, the M and L vibrations become excited to different extents, which depend on detailed intermolecular couplings. Let the subscript i denote vibrations in the M tier and the subscript j, vibrations in the L tier. Then ϕ_{PMi} is the quantum efficiency for IVR from P to mode i of the M tier, and ϕ_{PLj} is the quantum efficiency from P to mode j of the L tier.

In the second stage, two processes occur simultaneously: M → L and L → ground-state G. The time constants for M → L transfer are assumed in the absence of contradictory evidence to be approximately equal, so energy is transferred from the M tier to the L tier with a single time constant, $\tau_{ML} = (k_{ML})^{-1}$. The quantum efficiency for transfer from mode i of the M tier

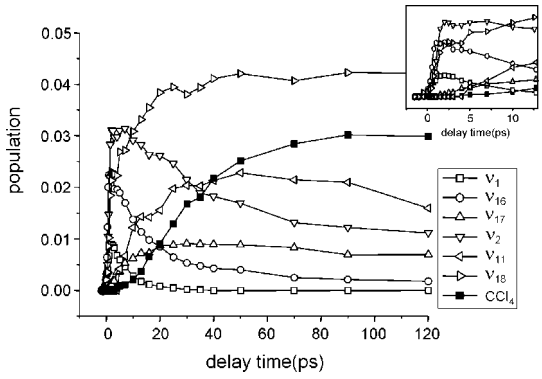

Figure 6. Population transients for benzene + 17% CCl_4 (v/v) determined using time-dependent Stokes and anti-Stokes spectra.

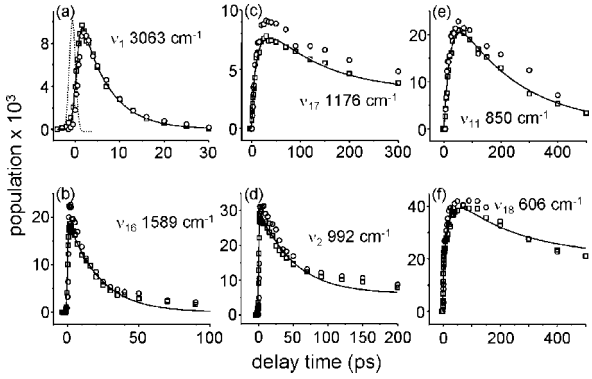

Figure 7. Comparison of population transients for neat benzene (squares) and benzene + 17% CCl_4 (v/v) (circles).

to mode j of the L tier is ϕ_{MiLj}. However, we do not experimentally determine which specific M vibration excites a specific L vibration, so we can measure only the net quantum efficiency of transfer *from all M modes* to mode L_i, φ_{MLj} $\sum_i M_i(t) = \sum_i \varphi_{MiLj} M_i(t)$. The L → G process is similarly treated by a single time constant, $\tau_{LG} = (k_{LG})^{-1}$.

The third stage commences as second-generation L vibrations are created by decay of M vibrations. The third stage results in the L → G process.

The three-stage model is summarized by the following set of equations.[27]

$$\begin{aligned}
\frac{dP(t)}{dt} &= -k_{IVR}[P(t) - P^{eq}] + \alpha J(t) \\
\frac{dM_i(t)}{dt} &= k_{IVR}\varphi_{PMi}[P(t) - P^{eq}] - k_{ML}[M_i(t) - M_i^{eq}] + \\
&\qquad \alpha'_i J(t) \\
\frac{dL_j(t)}{dt} &= k_{IVR}\varphi_{PLj}[P(t) - P^{eq}] + k_{ML}\varphi_{MLj}\sum_i [M_i(t) - \\
&\qquad M_i^{eq}] - k_{LG}[L_j(t) - L_j^{eq}] + \alpha''_j J(t)
\end{aligned} \tag{3}$$

In eqs 3, the superscript "eq" denotes thermal equilibrium population at the final temperature, T_f. $J(t)$ is the intensity of the IR pump pulse, and α is the IR absorption coefficient. The parameters α′ and α″ characterize the rates at which M or L vibrations, respectively, become excited by coherent interactions with P. Although we determine the quantum efficiencies ϕ_{PMi}, ϕ_{PLj}, and ϕ_{MLj} directly, since we do not detect many of the molecular vibrations, we have found it convenient to normalize the *observed vibrational energy* using the conditions $\Sigma\phi_{PMi} + \Sigma\phi_{PLj} = 1$ and $\Sigma\phi_{MLj} = 1$.[27] By way of example, if we observe two M vibrations and one L vibration having the same quantum efficiency for transfer, then $\phi = 0.33$ for each vibration, even though a great deal of energy might also be present in unobserved vibrations.

B. Ultrafast Raman Calorimetry. In the benzene−CCl_4 experiments, we observed the part of the benzene vibrational energy, $E_{obs}(t)$, in the strongly Raman-active vibrations. We also know the total energy input to the system, which can be computed either from the IR pulse properties and sample absorption coefficient or more conveniently from ΔT and the solution heat capacity. The CCl_4 molecular thermometer measures the rate that energy is dissipated into the bath.[4] The lower-frequency continuum of collective bath states of the solution is strongly coupled to the lowest frequency E-symmetry CCl_4 vibrations[4] so that CCl_4 becomes excited within a few picoseconds, allowing the molecular thermometer to respond quickly to a buildup of bath excitation. By properly normalizing the total energy, the observed energy, and the bath energy, we can determine by energy conservation how much energy resides in the invisible benzene vibrations. This ultrafast Raman calorimetry determination of the invisible vibrational energy, $E_{invis}(t)$, is an obvious idea, but until now, we did not have good enough data to implement it.

When energy is input by an IR pulse to a solution of benzene and CCl_4 at ambient temperature, after thermalization a temperature jump, ΔT, is created. The magnitude of ΔT is known from the data in Figures 8 and 11. For a δ-function excitation, the total energy increase corresponding to a particular value of ΔT would be

$$\begin{aligned}
\Delta E_{tot}(t) &= 0 \qquad t < 0 \\
\Delta E_{tot}(t) &= C_{tot}\Delta T \quad t \geq 0
\end{aligned} \tag{4}$$

where C_{tot} is the heat capacity of the solution. Given the quality of anti-Stokes data, we felt it was adequate to assume that $C_{tot} = C_{benzene} + C_{CCl_4}$, and that C_{tot} could be treated as constant, despite the temperature jump and the associated pressure jump and small volume expansion. We used tabulated heat capacity data.[48] Let $P(t)$ be the laser apparatus function, a Gaussian with fwhm of 1.4 ps normalized so that $\int P(t)\,dt = 1$. Then the time-dependent total energy increase with this finite-duration pulse would be

$$\Delta E_{tot}(t) = \int_{-\infty}^{t} P(t')\,\Delta E_{tot}(t')\,dt' \tag{5}$$

The solution is now taken to consist of two parts, a "system" of benzene vibrations and a "bath" of everything else: the lower-energy continuum of collective states of the two-component solution plus CCl_4 vibrations. Then the heat capacity of the bath C_{bath} can be written as

$$C_{bath} = C_{tot} - \sum_{i=1}^{n}\left(\frac{h\nu_i}{k_B T}\right)\frac{\exp(-h\nu_i/k_B T)}{[1 - \exp(-h\nu_i/k_B T)]^2} \tag{6}$$

where the sum is over all benzene vibrations ($n = 30$). To determine C_{bath}, once again avoiding the complications of a temperature-dependent heat capacity, eq 6 was evaluated at the temperature $T_i + \Delta T/2$. The benzene vibrational frequencies ν_i were obtained from the literature.[49]

The normalized time response of the CCl_4 molecular thermometer is denoted $T_{th}(t)$, where $T_{th}(t)$ is zero before the IR pulse and unity at long time. Then the time-dependent energy in the bath is given by

$$E_{bath}(t) = T_{th}(t)\,C_{bath}\Delta T \tag{7}$$

and the invisible vibrational energy is given by

$$E_{\text{invis}}(t) = E_{\text{tot}}(t) - E_{\text{obs}}(t) - E_{\text{bath}}(t) \quad (8)$$

In Figures 12 and 13, we have plotted $E_{\text{tot}}(t)$, $E_{\text{obs}}(t)$, $E_{\text{bath}}(t)$, and $E_{\text{invis}}(t)$ for benzene and benzene-d_6.

C. Benzene Vibrational Energy. Figure 12 shows benzene vibrational energy after IR CH-stretch pumping. The buildup of bath energy monitored by CCl_4 does not commence until a time delay of ~5 ps, which is consistent with the 6 ps parent decay representing an IVR process that does not involve dissipation into the bath. We do not believe this time delay is caused by a sluggish response of the molecular thermometer, since a significantly faster CCl_4 response was observed previously in a study of acetonitrile.[18] The half-life for the bath buildup is 30 ps, and thermalization is essentially complete by 100 ps. Even though the ν_{11} and ν_{18} vibrations have lifetimes in excess of 100 ps, these are lower-energy excitations, and after 100 ps, their aggregate contribution to the total dissipated energy is small. This measurement of the benzene vibrational cooling process should be considered more accurate than the previous study.[44]

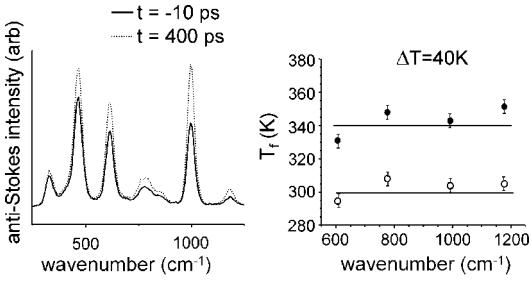

Figure 8. (left) Anti-Stokes spectra of benzene + 17% CCl_4 (v/v) at −10 ps prior to the IR pump pulse when the solution is in equilibrium at ambient temperature and at 400 ps after the IR pump pulse when the solution has thermalized. (right) Determination of ΔT. Solid circle is calculated temperature using 400 ps data, and open circle is calculated temperature using −10 ps data as reference.

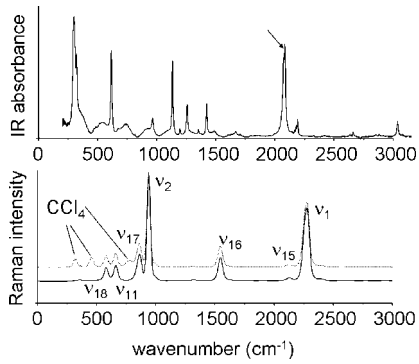

Figure 9. IR and Raman spectra of benzene-d_6 and Raman spectrum of benzene-d_6 with 17% CCl_4. The arrow indicates the wavenumber of the pump pulse. The Raman spectra are artificially broadened due to the 25 cm^{-1} bandwidth of the 532 nm laser pulses. The assignments are summarized in Table 1.

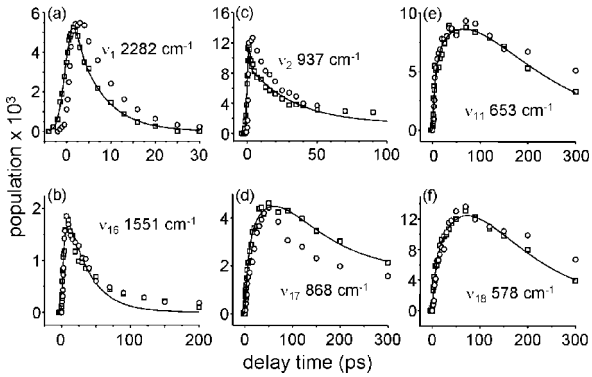

Figure 10. Comparison of population transients for neat benzene-d_6 (squares) and benzene-d_6 + 17% CCl_4 (v/v) (circles).

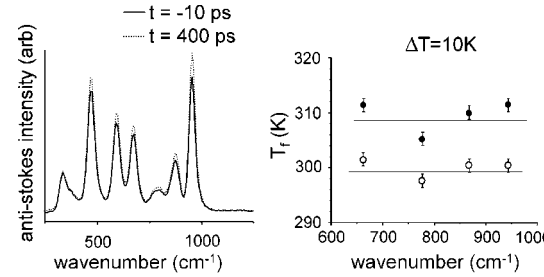

Figure 11. (left) Anti-Stokes spectra of benzene-d_6 + 17% CCl_4 (v/v) at −10 ps prior to the IR pump pulse when the solution is in equilibrium at ambient temperature and at 400 ps after the solution has thermalized. (right) Determination of ΔT. Solid circle is calculated temperature using 400 ps data, and open circle is calculated temperature using −10 ps data as reference.

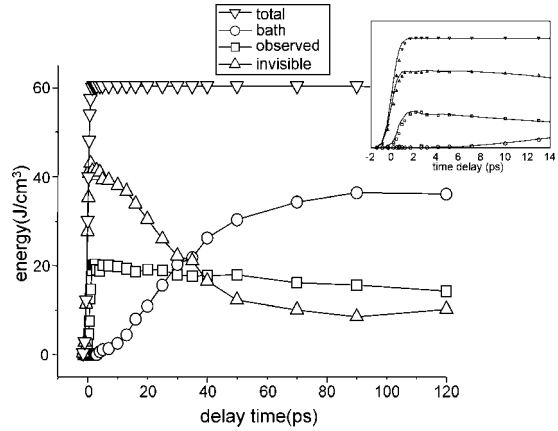

Figure 12. Ultrafast Raman calorimetry of benzene + 17% (v/v) CCl_4. The total energy input rises with the apparatus time response. The observed vibrational energy is the sum of the energy in 10 Raman-active vibrations probed by Raman. The bath, consisting of all excitations except the benzene vibrations, is probed using the CCl_4 molecular thermometer. The bath energy is determined using the long-time tail and the solution heat capacity. The invisible energy is the unobserved energy in benzene vibrations, determined using energy conservation. The inset shows the different rise times for E_{obs}, E_{invis}, and E_{bath}.

In Figure 12 (inset), the rising edge of $E_{\text{invis}}(t)$ is clearly faster than the rise of $E_{\text{obs}}(t)$, and at a shorter delay time of 2−3 ps immediately after the IR pulse stops pumping the benzene, the ratio of energies $E_{\text{invis}}/E_{\text{obs}} = 2.1$. At the very beginning, the IR pulse is directly pumping more energy into the invisible vibrations, and by 3 ps, about twice as much energy has been pumped into the invisible vibrations as into the observed vibrations. This might be expected, since the IR pulse is pumping IR-active vibrations near 3050 cm^{-1}, such as ν_{12}, while we are probing IR-inactive vibrations such as ν_1 and ν_2. In other words the coherent admixture of normal modes that constitutes the bright state has about twice as much of the IR-active mode character as the IR-inactive mode character. The decay rate of $E_{\text{invis}}(t)$ seen in Figure 12 is perhaps 50% faster than $E_{\text{obs}}(t)$.

In the benzene experiments, the number of observed vibrations was 10 and the total number of vibrations was 30. We observed 33% of the vibrations, and the maximum value of $E_{\text{obs}}/E_{\text{tot}}$ (from Figure 12) was also 33%. So in benzene, the amount of vibrational energy per mode is the same in the strongly Raman-active "observed" vibrations as in the "invisible" vibrations.

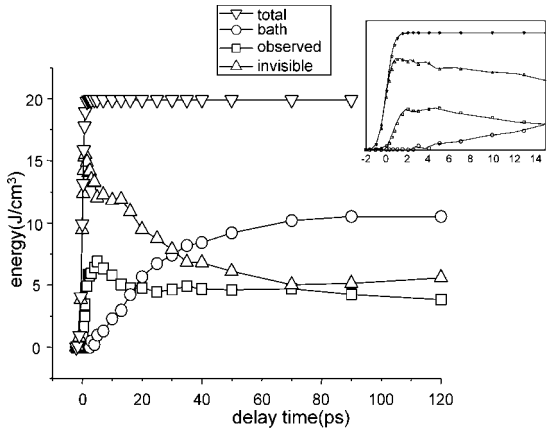

Figure 13. Anti-Stokes Raman calorimetry of benzene-d_6 + 17% (v/v) CCl_4 showing the total energy input by the IR pulses, the energy in the 12 observed benzene-d_6 vibrations, energy in the bath monitored with the CCl_4 molecular thermometer, and the invisible energy in benzene-d_6 vibrations not observed by Raman. The inset shows the different rise times for E_{obs}, E_{invis}, and E_{bath}.

D. Deuterobenzene Vibrational Energy. Figure 13 shows benzene-d_6 vibrational energy after CD-stretch pumping. In Figure 13, the rising edge of $E_{invis}(t)$ is again clearly faster than the rise of $E_{obs}(t)$, and at a shorter delay time of 2 ps, the ratio of energies is $E_{invis}/E_{obs} = 2.1$. That indicates that, as in benzene, the IR pulse is directly pumping twice as much energy into the invisible vibrations as into the observed vibrations. There is an ~5 ps time delay before the molecular thermometer begins to rise, indicating the decay of the parent CD-stretch is primarily intramolecular. The half-life of the bath buildup is noticeably shorter than in benzene, 20 ps as compared to 30 ps. Thermalization is essentially complete by 100 ps. The decay rates of $E_{invis}(t)$ and $E_{obs}(t)$ are similar enough to be indistinguishable. With benzene-d_6, the number of observed vibrations was 12, and the total number of vibrations was 30, so we observed 40% of the vibrations, and the maximum value of E_{obs}/E_{tot} (from Figure 13) was 36%. Thus, the amount of energy per vibration in benzene-d_6 is 10% less for the "observed" strongly Raman-active vibrations than for the "invisible" vibrations.

E. Benzene Vibrational Redistribution. The anti-Stokes transients for benzene were fit using eqs 3; the fitted curves are shown in Figure 7. The fitting parameters are listed in Table 1. The parent ν_1 has a lifetime of 6.2 (± 1) ps, in good agreement with a previous measurement[44] of 8 (± 1) ps, but we believe the present value is more accurate. The vibrations ν_1, ν_{16}, ν_2, and ν_{18} evidence an instantaneous rise due to IR laser pumping that was not resolved in earlier studies. The parent IVR process excites ν_{17} and ν_2 to roughly equal extents and ν_{18} to about one-half the level of the other two. Parent IVR does not excite ν_{11} at all.

On the basis of frequencies alone, we would guess that ν_{16} is the only midrange vibration being observed, whereas ν_{17}, ν_2, ν_{11} and ν_{18} are the lower-energy vibrations. This assignment is consistent with what we concluded from fitting the transients. Looking at the transients for ν_{17}, ν_2, ν_{11}, and ν_{18}, we see a significant contribution to the rise of ν_{11} and ν_{18} (Figures 4, 7e and 7f) that can be fit with a time constant close to the ν_{16} lifetime of 20 ps. We cannot tell if these lower-energy vibrations are populated from ν_{16} alone or from ν_{16} along with other midrange states nearby in energy having similar 20 ps lifetimes. The midrange-to-lower energy process populates mostly ν_{11} and ν_{18}, with <10% of the energy going into ν_{17}. The midrange to ν_2 process is essentially nonexistent. Three of the lower-energy vibrations have lifetimes longer than 100 ps, which is quite long by the standards of other polyatomic liquids.

F. Deuterobenzene Vibrational Redistribution. The anti-Stokes transients for benzene-d_6 were fit using eqs 3; the fitted curves are shown in Figure 10. The fitting parameters are listed in Table 1. The parent ν_1 has a lifetime of 6.4 (±1) ps, essentially the same as the CH-stretch of benzene. The other observed CD-stretch, ν_{15}, has a 4.5 ps lifetime. The ν_1, ν_{15}, and ν_2 vibrations evidence an instantaneous rise due to IR laser pumping. The parent IVR process excites ν_{11}, ν_{16}, ν_{17}, and ν_{18}, with ν_{11} and ν_{18} receiving the most excitation. It is interesting that parent IVR does not populate ν_2 in benzene-d_6, whereas there is significant population of this state by parent IVR in benzene.

Examine the rising edge of the lower-energy vibration ν_{18} in Figure 10. There is a slower component to the rise that is indicative of energy transfer from a higher-energy state that is quite long-lived, having a lifetime in the ~80 ps range. To a lesser extent, the same slow rise can also be seen in the ν_{11} and ν_{17} transients in Figure 10; however, the observed midrange vibrations have 25 ps lifetimes. To explain this ~80 ps time constant seen in rising edges but not in the decay of higher-energy vibrations, we postulate the existence of an unobserved state in the midrange tier that is feeding population relatively slowly to the lower-energy tier. We will call this state X. State X is excited with good efficiency by IVR from the parent CD-stretch, and when it decays, it populates the states at 868 cm^{-1} and below. Since state X must be higher in energy than 868 cm^{-1}, X seems likely to be a CD-bending mode or a ring-stretching mode. The X state decay pathway primarily involves populating ν_{18}. Thus, the model of all M vibrations having the same lifetime is not valid for benzene, since there are M vibrations with 80 and 25 ps lifetimes.

5. Summary and Conclusions

We have presented the most detailed investigation to date of vibrational energy dynamics in liquid benzene and the first investigation of vibrational energy in liquid benzene-d_6. Since these molecules have inversion symmetry, the IR pump must excite states that are Raman-inactive. The Raman intensity is concentrated into a small number (6−7) of transitions, of which many are doubly degenerate. Still, we observe only a fraction of the 30 vibrations, 33% in benzene and 40% in benzene-d_6. Using a CCl_4 molecular thermometer, we can monitor the total energy dissipated from vibrationally excited benzene to the bath and thereby infer the time-dependence of vibrational energy in the aggregate unobserved vibrations. The detailed vibration-to-vibration relaxation pathways were analyzed in the context of a three-state model described previously, keeping in mind that the rigid molecular framework might give rise to relaxation pathways that are more specific than what was previously observed in other species, such as nitromethane[5] or glycine in aqueous solution.[24,27]

Our measurements show that the parent excitations in benzene and benzene-d_6, nominally a CH-stretch (3050 cm^{-1} pumping with ~40 cm^{-1} bandwidth) or CD-stretch excitation (2280 cm^{-1} pumping with ~40 cm^{-1} bandwidth), evidence a great deal of coherent coupling with other states, in which coherent coupling as described in the Introduction means the redistribution is faster than T_2. IR−Raman measurements have frequently observed this type of coupling with CH-bend and CD-bend vibrations[3] and occasionally with other vibrations at about one-half the parent frequency, such as NO_2's stretching of CH_3NO_2,[5] but the number of strongly coupled modes we observe by anti-

Stokes Raman is much greater in benzene then in any other molecule yet studied. Additionally, the ultrafast calorimetry data indicate that even more of the pump pulse energy is coherently coupled to the invisible vibrations. It is also the case that the VR pathways appear to be more specific than in other molecules studied to date, by which we specifically mean certain vibrations are simply bypassed in one or more stages of the three-stage model. As seen in Table 1, the parent IVR stage in benzene does not excite ν_{11}, and the midrange-to-lower energy stage does not excite ν_2. In benzene-d_6, the parent IVR stage does not excite ν_2, and the midrange-to-lower energy stage does not excite either ν_2 or ν_{17}.

We observe only 33% or 40% of the benzene or benzene-d_6 vibrations, but we compensate in part with ultrafast calorimetry, which provides some new insights into the question of whether observing just the Raman-active vibrations provides an accurate picture of benzene vibrational cooling. In benzene-d_6, this is clearly true. The average energy (per mode) is within 10% in observed and invisible vibrations, and the decay rates are quite similar. In benzene, this is almost true. The average energy per mode is the same in both observed and invisible vibrations, but the invisible vibrational energy decays somewhat faster. The slower decay of energy from Raman-active vibrations in benzene but not in benzene-d_6 is consistent with many low-temperature coherent Raman studies of crystalline naphthalene,[42,50−53] anthracene,[51] and pentacene,[54,55] which showed that A_g vibrations, also those with the largest Raman cross sections, had significantly longer lifetimes in the proto but not in the deutero species.[56]

One point worth emphasizing is the very different timescales for decay of the initial state, ~6 ps, and the overall vibrational cooling process.[57] The cooling process is characterized by a half-life of 30 (20) ps in benzene (benzene-d_6), and there is clear evidence for vibrationally hot molecules, even at 80 ps.

References and Notes

(1) Laubereau, A.; Kaiser, W. *Rev. Mod. Phys.* **1978**, *50*, 607.

(2) Deàk, J. C.; Iwaki, L. K.; Rhea, S. T.; Dlott, D. D. *J. Raman Spectrosc.* **2000**, *31*, 263.

(3) Iwaki, L. K.; Deàk, J. C.; Rhea, S. T.; Dlott, D. D. Vibrational energy redistribution in polyatomic liquids: Ultrafast IR−Raman spectroscopy. In *Ultrafast Infrared and Raman Spectroscopy*; Fayer, M. D., Ed.; Marcel Dekker: New York, 2000; p 541.

(4) Graham, P. B.; Matus, K. J. M.; Stratt, R. M. *J. Chem. Phys.* **2004**, *121*, 5348.

(5) Shigeto, S.; Pang, Y.; Fang, Y.; Dlott, D. D. *J. Phys. Chem. B* **2008**, *112*, 232.

(6) Deàk, J. C.; Rhea, S. T.; Iwaki, L. K.; Dlott, D. D. *J. Phys. Chem. A* **2000**, *104*, 4866.

(7) Pakoulev, A.; Wang, Z.; Dlott, D. D. *Chem. Phys. Lett.* **2003**, *371*, 594.

(8) Pakoulev, A.; Wang, Z.; Pang, Y.; Dlott, D. D. *Chem. Phys. Lett.* **2003**, *380*, 404.

(9) Wang, Z.; Pakoulev, A.; Pang, Y.; Dlott, D. D. *J. Phys. Chem. A* **2004**, *108*, 9054.

(10) Wang, Z.; Pang, Y.; Dlott, D. D. *J. Chem. Phys.* **2004**, *120*, 8345.

(11) Wang, Z.; Pang, Y.; Dlott, D. D. *Chem. Phys. Lett.* **2004**, *397*, 40.

(12) Wang, Z.; Pang, Y.; Dlott, D. D. *J. Phys. Chem. B* **2006**, *110*, 201150.

(13) Wang, Z.; Pang, Y.; Dlott, D. D. *J. Phys. Chem. A* **2007**, *111*, 3196.

(14) Hofmann, M.; Graener, H. *Chem. Phys.* **1995**, *206*, 129.

(15) Graener, H.; Laubereau, A. *Chem. Phys. Lett.* **1983**, *102*, 100.

(16) Graener, H.; Zürl, R.; Hofmann, M. *J. Phys. Chem.* **1997**, *101*, 1745.

(17) Deàk, J. C.; Iwaki, L. K.; Dlott, D. D. *Chem. Phys. Lett.* **1998**, *293*, 405.

(18) Deàk, J. C.; Iwaki, L. K.; Dlott, D. D. *J. Phys. Chem.* **1998**, *102*, 8193.

(19) Deàk, J. C.; Iwaki, L. K.; Dlott, D. D. *J. Phys. Chem. A* **1999**, *103*, 971.

(20) Ambroseo, J. R.; Hochstrasser, R. M. *J. Chem. Phys.* **1988**, *89*, 5956.

(21) Ambroseo, J. R.; Hochstrasser, R. M. Vibrational relaxation pathways of the N-H stretch of pyrrole in liquids. In *Ultrafast Phenomena VI*; Yajima, T., Yoshihara, K., Harris, C. B., Shionoya, S., Eds.; Springer-Verlag: Berlin, Heidelberg, 1988; Vol. 48; p 450.

(22) Iwaki, L. K.; Dlott, D. D. *Chem. Phys. Lett.* **2000**, *321*, 419.

(23) Iwaki, L. K.; Dlott, D. D. *J. Phys. Chem. A* **2000**, *104*, 9101.

(24) Shigeto, S.; Dlott, D. D. *Chem. Phys. Lett.* **2007**, *447*, 134.

(25) Iwaki, L.; Dlott, D. D. Vibrational energy transfer in condensed phases. In *Encyclopedia of Chemical Physics and Physical Chemistry*; Moore, J. H., Spencer, N. D., Eds.; IOP Publishing Ltd.: London, 2001; p 2717.

(26) Hoffman, G. J.; Imre, D. G.; Zadoyan, R.; Schwentner, N.; Apkarian, V. A. *J. Chem. Phys.* **1993**, *98*, 9233.

(27) Fang, Y.; Shigeto, S.; Seong, N.-H.; Dlott, D. D. *J. Phys. Chem. B* **2008**, . in press.

(28) Nitzan, A.; Jortner, J. *Mol. Phys.* **1973**, *25*, 713.

(29) Felker, P. M.; Zewail, A. H. *Phys. Rev. Lett.* **1984**, *53*, 501.

(30) Tokmakoff, A.; Kwok, A. S.; Urdahl, R. S.; Francis, R. S.; Fayer, M. D. *Chem. Phys. Lett.* **1995**, *234*, 289.

(31) Tanabe, K.; Jonas, J. *Chem. Phys. Lett.* **1977**, *53*, 278.

(32) Stewart, G. M.; McDonald, J. D. *J. Chem. Phys.* **1983**, *83*, 3907.

(33) Callegari, A.; Srivastava, H. K.; Merker, U.; Lehmann, K. K.; Scoles, G.; Davis, M. J. *J. Chem. Phys.* **1997**, *106*, 432.

(34) Reddy, K. V.; Heller, D. F.; Berry, M. J. *J. Chem. Phys.* **1982**, *76*, 2814.

(35) Sibert, E. L., III.; Hynes, J. T.; Reinhardt, W. P. *J. Chem. Phys.* **1984**, *81*, 1135.

(36) Sibert, E. L., III.; Reinhardt, W. P.; Hynes, J. T. *Chem. Phys. Lett.* **1982**, *92*, 455.

(37) Sibert, E. L., III.; Reinhardt, W. P.; Hynes, J. T. *J. Chem. Phys.* **1984**, *81*, 1115.

(38) Ho, F.; Tsay, W.-S.; Trout, J.; Velsko, S.; Hochstrasser, R. M. *Chem. Phys. Lett.* **1983**, *97*, 141.

(39) Velsko, S.; Hochstrasser, R. M. *J. Phys. Chem.* **1985**, *89*, 2240.

(40) Neuman, M. N.; Tabisz, G. C. *Chem. Phys.* **1976**, *15*, 195.

(41) Trout, T. J.; Velsko, S.; Bozio, R.; Decola, P. L.; Hochstrasser, R. M. *J. Chem. Phys.* **1984**, *81*, 4746.

(42) Decola, P. L.; Hochstrasser, R. M.; Trommsdorff, H. P. *Chem. Phys. Lett.* **1980**, *72*, 1.

(43) Fendt, A.; Fischer, S. F.; Kaiser, W. *Chem. Phys.* **1981**, *57*, 55.

(44) Iwaki, L. K.; Deàk, J. C.; Rhea, S. T.; Dlott, D. D. *Chem. Phys. Lett.* **1999**, *303*, 176.

(45) Chen, S.; Hong, X.; Hill, J. R.; Dlott, D. D. *J. Phys. Chem.* **1995**, *99*, 4525.

(46) Chen, S.; Tolbert, W. A.; Dlott, D. D. *J. Phys. Chem.* **1994**, *98*, 7759.

(47) Oxtoby, D. W. Vibrational population relaxation in liquids. In *Photoselective Chemistry, Part 2*; Jortner, J., Levine, R. D., Rice, S. A., Eds.; Wiley: New York, 1981; Vol. 47, p 487.

(48) Watanabe, H.; Kato, H. *J. Chem. Eng. Data* **2004**, *49*, 809.

(49) Shimanouchi, T. *Tables of Molecular Vibrational Frequencies. Consolidated, Volume I*; U.S. Government Printing Office: Washington, D. C., 1972.

(50) Hill, J. R.; Chronister, E. L.; Chang, T.-C.; Kim, H.; Postlewaite, J. C.; Dlott, D. D. *J. Chem. Phys.* **1988**, *88*, 949.

(51) Schosser, C. L.; Dlott, D. D. *J. Chem. Phys.* **1984**, *80*, 1394.

(52) Bellows, J. C.; Prasad, P. N. *J. Chem. Phys.* **1979**, *70*, 1864.

(53) Hesp, B. H.; Wiersma, D. A. *Chem. Phys. Lett.* **1980**, *75*, 423.

(54) Hill, J. R.; Chronister, E. L.; Chang, T.-C.; Kim, H.; Postlewaite, J. C.; Dlott, D. D. *J. Chem. Phys.* **1988**, *88*, 2361.

(55) Hesselink, W. H.; Wiersma, D. A. *J. Chem. Phys.* **1980**, *73*, 648.

(56) Dlott, D. D. Dynamics of molecular crystal vibrations. In *Laser Spectroscopy of Solids II*; Yen, W., Ed.; Springer Verlag: Berlin, 1988; p 167.

(57) Hill, J. R.; Dlott, D. D. *J. Chem. Phys.* **1988**, *89*, 830.

JP809679Y